

# SI-POFs frequency response obtained by solving the power flow equation

M<sup>a</sup> Ángeles Losada, Javier Mateo, Juan J. Martínez and Alicia López

**Abstract**—We present a method to derive the space-time evolution of the angular power distribution when it is transmitted throughout large core step index (SI) plastic optical fibers (POFs). The model is based on the power flow equation generalized to introduce the temporal dimension where the diffusion and attenuation of the fibers are given by functions of the propagation angle. To solve this equation we propose a fast implementation of the finite-difference method in matrix form. We calculate model predictions for the fiber frequency response versus length and then, compare them to experimental data. We found that angular diffusion has a strong impact on temporal pulse widening with propagation. Thus, a better understanding of power propagation can prove very useful in increasing the bandwidth of POF links in real situations.

**Index Terms**—SI-POF diffusion model, Power Flow equation, Frequency response.

## I. INTRODUCTION

MULTIMODE fibers transmission properties (attenuation and bandwidth) show non-linear changes with propagation length whose origin is attributed to mode coupling. In fact, the concatenation factor is an empirical parameter widely used when estimating the fiber maximum span for a given data rate. Plastic optical fibers, with highly multimode transmission and strong mode coupling, show a complex relationship between bandwidth and length different from ray-theory predictions [1]. In the literature there are several proposals to obtain bandwidth from other parameters such as numerical aperture (NA) [2]. We showed in previous studies that this model cannot give a complete description of the changes in bandwidth with length.

In another work, we devised a method based on Gloge's power flow equation and on experimental far field patterns

(FFPs) to obtain the angular diffusion and attenuation functions characteristic of a given fiber [3]. These functions provide an overall description of the fiber behavior and, along with the power flow equation, can be used to predict output power angular distributions at any fiber lengths and for any launching conditions [4].

Here, we propose the use of Gloge's generalization of the differential power flow equation to obtain the pulse temporal spread with propagation [5]. The temporal dependence is introduced into the equation which is then solved in the temporal frequency domain using a fast matrix approach of the finite-difference method for the given angular diffusion and attenuation functions. In this way, the frequency response can be obtained for each particular fiber at a range of lengths. To verify the model, these estimates have been compared to frequency response functions measured for the same fibers and conditions than the FFPs used to determine the angular diffusion and attenuation.

In this paper, we first briefly describe the experimental setup and methods to obtain the FFPs and frequency responses versus length for the tested POFs. Second, we describe our model based on Gloge's differential equation and the fast procedure devised to solve it. Third, we present the results, comparing the experimental and predicted frequency responses. Afterwards, we discuss the model predictions that can be applied to design configurations that optimize POF behavior in real links. Finally, we summarize the conclusions.

## II. EXPERIMENTAL METHODS

We measured the frequency response and FFP versus fiber length for three PMMA fibers of 1mm diameter from different manufacturers: ESKA-PREMIER GH4001 (GH) from Mitsubishi, HFBR-RUS100 (HFB) from Agilent, and PGU-FB1000 (PGU) from Toray. The GH and PGU fibers have a NA of 0.5, corresponding to a 19.5° inner critical angle. The HFB fiber has a NA of 0.47 which implies an 18.5° inner critical angle. For each fiber both the FFP and frequency responses were measured under the same launching conditions, taken sequentially starting from a long fiber (175m-100m) down to 10m. We measured the frequency response at each length using a frequency method which consists on sweeping the frequency of a pure sinusoidal waveform that is fed to an AlGaInP laser diode (LD SANYO DL-3147-021) emitting a maximum of 5mW at 645nm and with a typical divergence of 30° in the perpendicular plane,

Manuscript received July 4, 2008. This work was supported by the Spanish Ministry for Science and Technology under grant TEC2006-13273-C03-02.

M. A. Losada is with the Group of Photonic Technology, Aragón Institute of Engineering Research (i3A), University of Zaragoza, María de Luna 1, 50018 Zaragoza, Spain. (phone: +34 976762373. fax: +34 976762111. e-mail: alosada@unizar.es).

J. Mateo is with the Group of Photonic Technology, Aragón Institute of Engineering Research (i3A), University of Zaragoza. (e-mail: jmateo@unizar.es).

J. J. Martínez is with the University of Zaragoza. (e-mail: jjosemar@unizar.es).

A. López is with the Group of Photonic Technology, Aragón Institute of Engineering Research (i3A), University of Zaragoza. (e-mail: aliclope@unizar.es).

and of  $7.5^\circ$  in the parallel plane [6]. The receptor is based on a 1mm diameter photodiode (FDS010) whose output is amplified using a 40dB amplifier (Mini-Circuits ZKL-1R5) with a band-pass from 10MHz to 1.5GHz. A wideband Infinium DCA 86100A oscilloscope from Agilent is connected to the output of the amplifier and captures the received signal whose amplitude is directly related with the frequency response of the system. The devices are fully controlled and data is acquired by the computer through the GPIB and processed to make our method more robust and to extend the bandwidth measurements far above the system bandwidth (up to 1GHz). The frequency response of a short segment of fiber (75cm) is obtained to be used as a reference to characterize the effect of the electrical components. At the same time, the FFP images were captured using a set-up which has been thoroughly described elsewhere [3, 7].

### III. THEORY

We use Gloge's power flow equation to describe the evolution of the modal power distribution as it is transmitted throughout a POF where different modes are characterized by their propagation angle with respect to fiber axis ( $\theta$ ), which can be taken as a continuous variable [3, 5]. We make no assumptions about the angular diffusion,  $d(\theta)$ , and attenuation,  $\alpha(\theta)$ , which are described as functions of  $\theta$ . Following the procedure described in [5], we introduce the temporal dimension and, given that  $dt/dz = n/(c \cos \theta)$ , we obtain the following equation:

$$\frac{\partial P(\theta, z, t)}{\partial z} = -\alpha(\theta)P(\theta, z, t) - \frac{n}{c \cos \theta} \cdot \frac{\partial P(\theta, z, t)}{\partial t} + \frac{1}{\theta} \frac{\partial}{\partial \theta} \left( \theta \cdot d(\theta) \cdot \frac{\partial P(\theta, z, t)}{\partial \theta} \right). \quad (1)$$

Then, we take the Fourier transform at both sides of equation (1) and use the Fourier derivation property to obtain the following simplified equation:

$$\frac{\partial p(\theta, z, \omega)}{\partial z} = -\left( \alpha(\theta) + \frac{n}{c \cos \theta} \cdot j\omega \right) p(\theta, z, \omega) + \frac{1}{\theta} \frac{\partial}{\partial \theta} \left( \theta \cdot d(\theta) \cdot \frac{\partial p(\theta, z, \omega)}{\partial \theta} \right), \quad (2)$$

where  $p(\theta, z, \omega) = \int_{-\infty}^{+\infty} \exp(-j\omega t) P(\theta, z, t) dt$  is the Fourier transform of  $P(\theta, z, t)$ .

To solve this differential equation we implement a finite-difference method where we use a forward difference for the first angular derivative at  $\theta$ , and a second-order central difference for the second derivative, obtaining the power at angle  $\theta$  and distance  $z + \Delta z$  as the combination of the power at the same angle and the two adjacent angles ( $\theta + \Delta\theta$ ,  $\theta - \Delta\theta$ ) at distance  $z$  as shows the resulting equation:

$$p(\theta, z + \Delta z, \omega) = \left( 1 - \left( \alpha(\theta) + \frac{n}{c \cos \theta} \cdot j\omega \right) \Delta z \right) p(\theta, z, \omega) + \frac{\Delta z}{2 \cdot \Delta\theta} \left( \frac{d(\theta)}{\theta} + d'(\theta) \right) \left( p(\theta + \Delta\theta, z, \omega) - p(\theta - \Delta\theta, z, \omega) \right) - \frac{2d(\theta)\Delta z}{\Delta\theta^2} p(\theta, z, \omega) + \frac{d(\theta)\Delta z}{\Delta\theta^2} \left( p(\theta + \Delta\theta, z, \omega) + p(\theta - \Delta\theta, z, \omega) \right). \quad (3)$$

For any pair of lengths,  $z_2 > z_1$ , we can put the difference equation in matrix notation as:

$$p(\theta, z_2, \omega) = (\mathbf{A}(\omega) + \mathbf{D})^{\frac{z_2 - z_1}{\Delta z}} \cdot p(\theta, z_1, \omega). \quad (4)$$

$\mathbf{A}$  is a diagonal matrix that describes power propagation without diffusion and whose elements are given by:

$$A_{k,k}(\omega) \approx 1 - \Delta z \cdot \alpha(k \cdot \Delta\theta) - \Delta z \cdot \frac{n}{c \cos(k \cdot \Delta\theta)} \cdot j\omega, \quad (5)$$

which is the first order approximation of:

$$A_{k,k}(\omega) = \exp \left( -\Delta z \cdot \alpha(k \cdot \Delta\theta) - \Delta z \cdot \frac{n}{c \cos(k \cdot \Delta\theta)} \cdot j\omega \right). \quad (6)$$

Notice that  $\mathbf{A}$  is the only frequency dependent term in the equation. For  $\omega=0$ , the solution of the equation is the FFP at a given length  $L$ ,  $P(\theta, z=L)$ . Iteration over the values of  $\omega$  gives the complete spatial and temporal evolution of the optical power in the fiber. The complex values of  $A_{k,k}(\omega)$  are obtained by sampling the angular frequency  $\omega$  as required for a precise calculation of the inverse discrete Fourier transform of  $p(\theta, z, \omega)$  to obtain  $P(\theta, z, t)$ .

The matrix  $\mathbf{D}$  is a tri-diagonal matrix which accounts for diffusion along the fiber. Its elements for  $k > 0$  are:

$$D_{k,k-1} = \left( d(k \cdot \Delta\theta) - \frac{1}{2} \frac{d(k \cdot \Delta\theta)}{k} - \frac{1}{2} d'(k \cdot \Delta\theta) \Delta\theta \right) \frac{\Delta z}{\Delta\theta^2} \\ D_{k,k} = -2d(k \cdot \Delta\theta) \frac{\Delta z}{\Delta\theta^2} \quad (7)$$

$$D_{k,k+1} = \left( d(k \cdot \Delta\theta) + \frac{1}{2} \frac{d(k \cdot \Delta\theta)}{k} + \frac{1}{2} d'(k \cdot \Delta\theta) \Delta\theta \right) \frac{\Delta z}{\Delta\theta^2}.$$

These matrix elements describe power diffusion through a differential length of the fiber indicating the fraction of power that flows out from a given angle, and the fraction that drifts to this angle from the adjacent ones. The undetermined value at  $k=0$  corresponding to  $\theta=0$ , is obtained by applying the approximation used in [8]:

$$\lim_{\theta \rightarrow 0} \frac{1}{\theta} \frac{\partial}{\partial \theta} \left( \theta \cdot \frac{\partial P(\theta, z)}{\partial \theta} \right) \approx 2 \lim_{\theta \rightarrow 0} \frac{\partial^2 P(\theta, z)}{\partial \theta^2}, \quad (8)$$

and the evenness property of  $P(\theta, z)$  with  $\theta$ , which result in:

$$D_{0,0} = -4d(0) \frac{\Delta z}{\Delta\theta^2} \quad D_{0,1} = 4d(0) \frac{\Delta z}{\Delta\theta^2}. \quad (9)$$

The other contour condition at the maximum  $k$ ,  $N$ , is:

$$D_{N,N-1} = 2d(N) \frac{\Delta z}{\Delta\theta^2} \quad D_{N,N} = -2d(N) \frac{\Delta z}{\Delta\theta^2}. \quad (10)$$

Matrix  $(\mathbf{A}(\omega)+\mathbf{D})$  carries all space-time information concerning power propagation through the fiber and thus, gives a complete description of the fiber as a transmission system. The key of the method we propose to solve equation (2) is to take advantage of the sparse nature of this matrix. Thus, to calculate multiple matrix powers is more efficient than to perform the same number of iterations, particularly when using MatLab<sup>®</sup>. Even more, it is not necessary to recalculate them when changing the initial condition to obtain the final space-time output power distribution. Once the initial condition is multiplied by the system matrix, it is possible to obtain the frequency response for each output angle,  $p(\theta, z, \omega)$ , as well as the global frequency response by integrating the total power for all angles at a given frequency:

$$p(L, \omega) = \int_{-\infty}^{+\infty} \sin(\theta) p(\theta, L, \omega) d\theta. \quad (11)$$

Its inverse Fourier transform gives the pulse spreading at this length,  $P(L, t)$ . The values of  $\Delta z$  and  $\Delta \theta$  that are critical for convergence have been determined according to the required precision. We have used  $\Delta z=0.001$  m and  $\Delta \theta=0.005$  rad obtaining accurate results.

#### IV. RESULTS

We introduced in the model the diffusion and attenuation functions,  $d(\theta)$  and  $\alpha(\theta)$ , previously estimated for the three different POFs [3] from experimental FFPs, to obtain the global frequency response versus length for each fiber. The experimental frequency responses, obtained in the same conditions than the FFPs, are shown in Figure 1 as circles for the three fibers: GH, in the upper graph; HFB, in the middle graph, and PGU, in the lower graph. In each graph, the different curves are the frequency responses at four different lengths: 10m, 20m, 65m and the longest tested length which was different for each fiber: 175m for GH; 100m for HFB and 150m for PGU. The frequency responses calculated using the model, are also represented in the plots as solid lines, showing that there is an overall good agreement between the predictions and the experimental data, particularly at the longest lengths given by the two bottom curves.

Moreover, the model allows us to obtain the output power distribution as a joint function of output angle and time at any fiber length,  $P(\theta, z, t)$  as the inverse Fourier transform of the calculated frequency response  $p(\theta, z, \omega)$ . The integrated power over the output angle results in the temporal pulse spread which has been normalized to represent it in the upper row of Figure 2 for the three fibers at the longest tested length. These functions are the inverse transform of the corresponding frequency responses shown in Figure 1. In the lower row, the power spread is represented as a joint function of output angle and time also for the longest fiber lengths  $P(\theta, z = L_{MAX}, t)$ . Time is shown on the horizontal axis in nanoseconds and output angle in degrees on the vertical axis. Power level is gray-scale coded darker for the higher levels and lighter for the lower level. Each horizontal section represents the temporal pulse arriving at a given output angle. Vertical

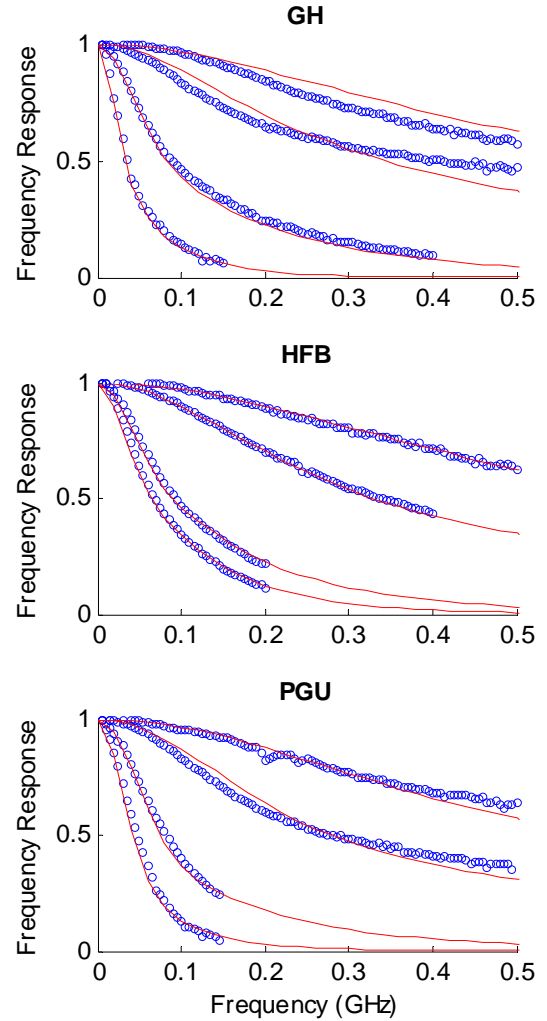


Fig. 1. Frequency responses for GH, HFB and PGU. Comparison of experimental measurements (circles) and model predictions (solid lines) for four lengths (10m, 20m, 65m and the longest measured fiber length)

sections are the radial profiles of the spatial power distribution at a fixed time. The integrated power over time gives the radial profile of the FFP which has been previously compared to the experimental FFPs [3]. The solid line over the image represents the delay at which the maximum power arrives at each output angle. The dashed line shows the delay obtained without diffusion given by the ray-theory inverse cosine law.

#### V. DISCUSSION

The graphs in Figure 1 with the experimental and model-predicted frequency responses show that the overall tendency is well captured by the model. However, there are some discontinuities in the experimental data which are not followed by the model predictions. These discontinuities arise from localized defects or strain in the fiber which, when removed by the cut-off procedure, let the remaining fiber recover its normal predictable behavior. Although the model is capable to include these effects, they are usually unknown and practically impossible to detect prior the measurements.

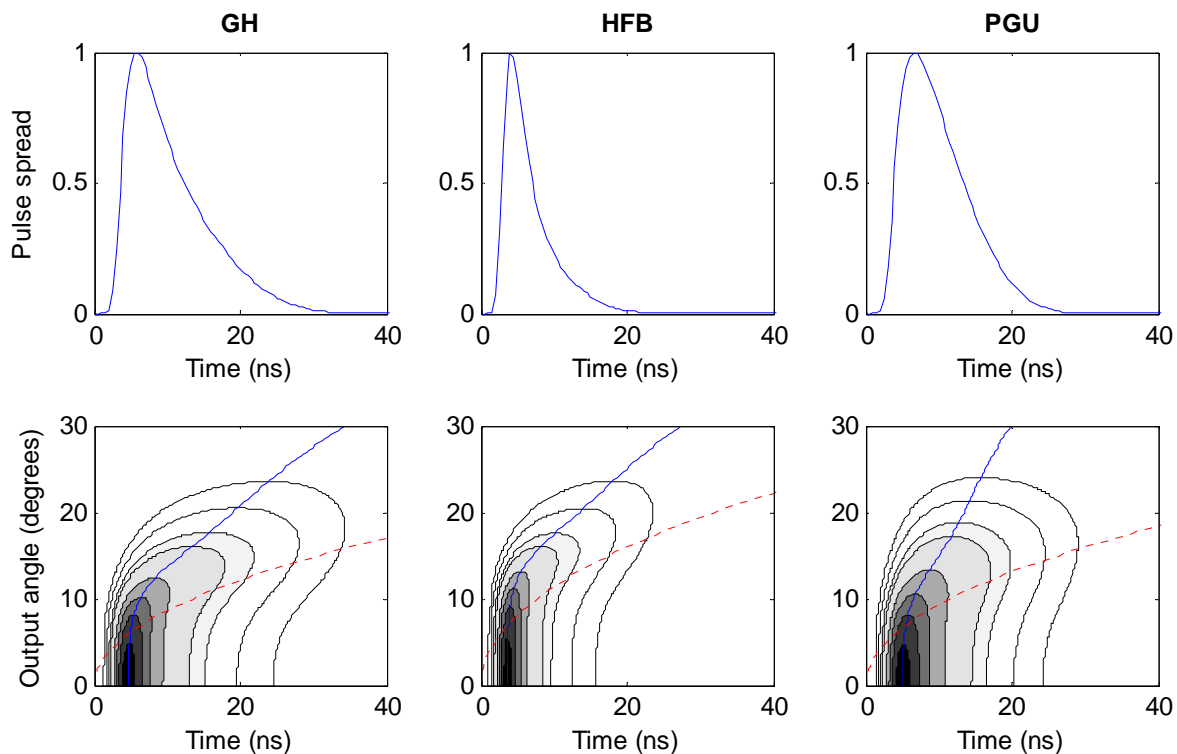


Fig. 2. Upper row: Overall pulse spread versus time. Lower row: Output power distribution as a function of output angle (vertical axis) and time (horizontal axis). Both figures are derived for the maximum tested fiber length: 175m for the GH (left), 100m for the HFB (middle) and 150m for the PGU fiber (right). The solid lines joint the delays for which the power is maximum at each output angle. The dashed lines give the delay in the absence of diffusion.

The upper row in Figure 2 shows the pulse time spread, which is the normalized inverse Fourier transform of the bottom curve in each graph of Figure 1. A common feature of these curves for all fibers is their asymmetry. Power rises first very steeply to its maximum and then, slowly decreases with a long tail which extends towards delays of 30 ns. There are, however, noticeable differences among fibers. For example, pulse spread for the HFB fiber is much narrower both in the peak and in the tail than those for the other two fibers, as corresponds to its wider frequency response in Figure 1.

The space-time distribution of the output power at the lower row of Figure 2 helps to understand the relationship between the angular power distribution and the pulse spreading through modal diffusion. The contour plots show how power at a range of low angles is concentrated at the shortest delays, while at higher angles the peak is at higher delays and there is a wider time spread. Although the overall shape is similar for all the fibers tested, the angular and temporal ranges are different and characteristic for each fiber type.

These effects are more clearly shown by the lines joining the maxima that start at a delay of a few nanoseconds, from 3 ns to 5 ns, depending on the fiber, following a nearly vertical line up to an angle between  $8^\circ$ - $10^\circ$  from where they start increasing. This increase is, however, steeper than the one given by the cosine prediction indicating longer delays for these angles in the absence of diffusion. These results support our previous findings consistent with diffusion mixing up the lower angles from the first fiber meters [9]. In this way, the vertical portion of the curve at low angles is explained by a

strong coupling that equalizes all the deterministic trajectories making all these angles to share an average trajectory. On the other hand, for higher angles the combined effect of diffusion and differential attenuation causes the power in higher angles to skew towards lower angles. This effect will shorten their delays and increase their differential attenuation relative to the case without diffusion.

Changes along the horizontal dimension show the evolution of the radial profile with time that can be exploited to improve the frequency response for a given fiber. The contour shape suggests an easy way to improve fiber capacity by spatial filtering out of the tail at the higher angles. Most power is confined in a range of lower angles, up to  $8^\circ$  for the GH and PGU fibers and  $10^\circ$  for the HFB, with the same peak delay and a narrow temporal spread. Thus, filtering out the power at the highest angles with a spatial filter will produce a narrower overall impulse response with small power loss.

We have recalculated the impulse response for 50 meters of the three fibers after filtering out the angular power above  $13.5^\circ$ . In Figure 3 the space-time power distributions at 50m are shown in the upper row in the same way as in Figure 2. The dashed line is the spatial filter cut-off of  $13.5^\circ$  which helps to visualize its effect. The lower row shows a comparison between the original (dashed lines) and the filtered frequency responses (solid lines), displaying a notable improvement for most frequencies. In fact, we have found this effect in our previous experimental measurements [10]. Table I gives the bandwidth before,  $BW_0$ , and after the filtering,  $BW_f$ , showing an increase up to 60MHz while the predicted power loss is

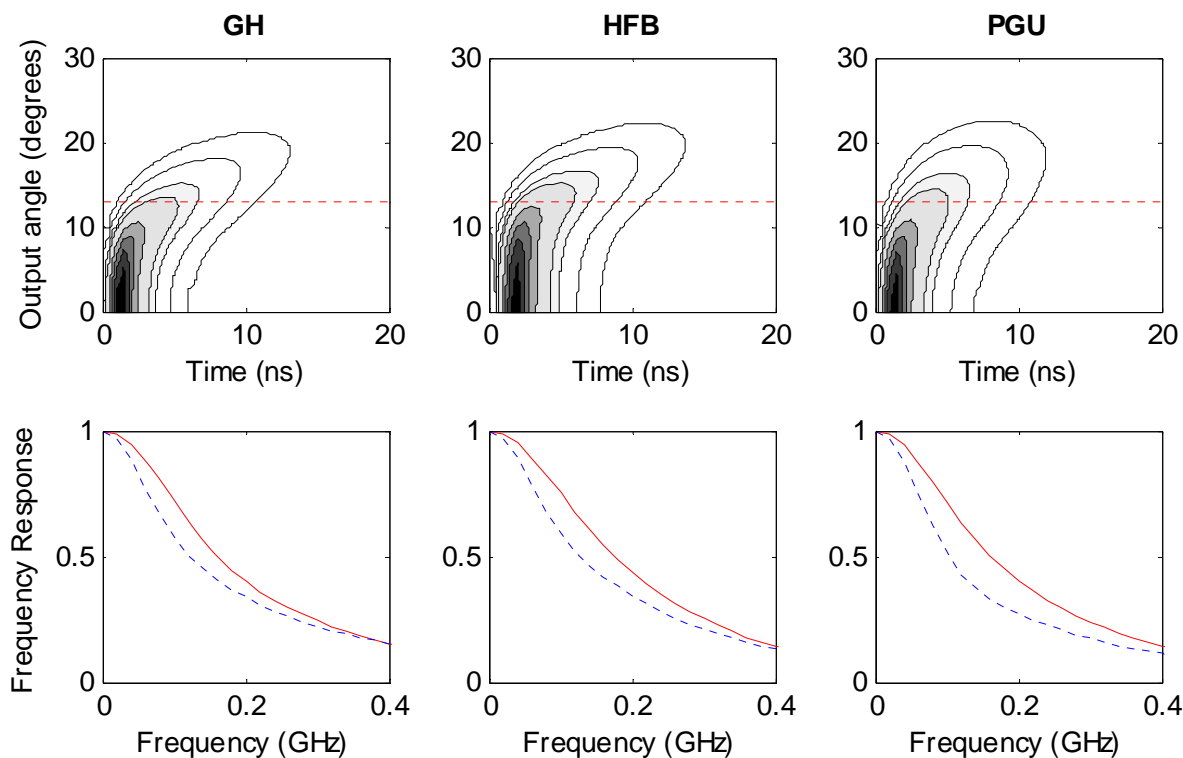


Fig. 3. Upper row: Output power distribution as a function of output angle (vertical axis) and time (horizontal axis) for a 50 meter length. Lower row: Comparison of original (dashed line) and filtered (solid line) frequency responses at 50 m. Data for GH is represented on the left, data for HFB is in the middle and PGU data, on the right.

always less than 3dB. In fact, the effect of the filter makes all three fibers viable for a Fast Ethernet link at 125 Mbps in 50m, while they were hardly able to reach this rate without filtering.

You can see that although all the power distributions in the upper row of Figure 3 have a similar tendency, the angular ranges are different for each fiber type, which suggests that the angular range for which strong diffusion occurs depends on fiber type and that it is possible to tailor the aperture diameter of the detector that maximizes the bandwidth without noticeably increasing the power loss.

TABLE I

SPATIAL FILTER EFFECT ON FIBER LOSS AND BANDWIDTH

	GH	HFB	PGU
Loss (dB)	1.84	2.67	2.68
$BW_0$ (MHz)	122	127	102
$BW_f$ (MHz)	161	176	161

## CONCLUSION

We propose a fast and robust method to obtain the space-time variation of optical power with propagation from which angular power distribution, attenuation, bandwidth and pulse spreading versus fiber length can be derived. We have verified the validity of the model by comparing model predictions with experimental results. Using the information provided by the space-time power distribution we found that fiber bandwidth

can be increased by an appropriate spatial filter, as we had shown experimentally before. Therefore, a good fiber characterization can be applied to optimize fiber performance in POF links.

## REFERENCES

- [1] J. Mateo, M. A. Losada, I. Garcés, J. Arrue, J. Zubia, and D. Kalymnios, "High NA POF Dependence of Bandwidth on Fibre Length," in Proc. 12th Int. Conf. POF'03, Seattle, USA, 2003, pp. 123-126.
- [2] D. Kalymnios, "Squeezing more bandwidth into high NA POF," in Proc. 8th Int. Conf. POF'99, Chiba, Japan, 1999, pp. 18-24.
- [3] J. Mateo, M.A. Losada, I. Garcés, and J. Zubia, "Global characterization of optical power propagation in step-index plastic optical fibers," Opt. Express 14, pp. 9028-9035, 2006.
- [4] M.A. Losada, J. Mateo, I. Garcés, and J. Zubia, "Estimation of the Attenuation and Diffusion Functions in Plastic Optical Fibers From Experimental far Field Patterns," in Proc. 15th Int. Conf. POF'06, Seoul, Korea, 2006, pp. 336-341.
- [5] D. Gloge, "Impulse Response of Clad Optical Multimode Fibers," B.S.T.J. 52, 801-816 (1973).
- [6] J. Mateo, M.A. Losada, J.J. Martínez-Muro, I. Garcés, and J. Zubia, "Bandwidth measurement in POF based on general purpose equipment," in Proc. 14th Int. Conf. POF'05, Honk-Kong, China 2005, pp. 53-56.
- [7] M.A. Losada, J. Mateo, D. Espinosa, I. Garcés, and J. Zubia, "Characterisation of the far field pattern for plastic optical fibres," in 13th Proc. Int. POF'04, Nuremberg, Germany, 2004, pp. 458-465.
- [8] M. Rousseau and L. Jeunhomme, "Numerical Solution of the Coupled-Power Equation in Step-Index Optical Fibers," IEEE Trans. Microwave Theory Tech., MIT-25, pp. 577-585, 1977.
- [9] M.A. Losada, J. Mateo, and L. Serena, "Analysis of propagation properties of step-index plastic optical fibers at non-stationary conditions," in Proc. 16th Int. POF'07, Torino, Italy, 2007, pp. 299-302.
- [10] P. Heredia, J. Mateo, and M.A. Losada, "Transmission capabilities of large core GI-POF based on BER measurements," in Proc. 16th Int. POF'07, Torino, Italy, 2007, pp. 307-310.